Osteoarthritis and Cartilage 32 (2024) 690–701

Osteoarthritis and Cartilage

Modulation of early osteoarthritis by tibiofemoral re-alignment in sheep

Jan Reinhard # [1], Tamás Oláh # † [1], Matthias W. Laschke ‡, Lars K.H. Goebel # †, Gertrud Schmitt #, Susanne Speicher-Mentges #, Michael D. Menger ‡, Magali Cucchiarini # †, Dietrich Pape † §, Henning Madry # † *

Center of Experimental Orthopaedics, Saarland University, 66421 Homburg, Germany
† *Cartilage Net of the Greater Region, 66421 Homburg, Germany*
‡ *Institute for Clinical and Experimental Surgery, Saarland University Medical Center and Saarland University, 66421 Homburg, Germany*
§ *Clinique d'Eich, Centre Hospitalier de Luxembourg, Eich, 1460 Luxembourg, Germany*

ARTICLE INFO

Article history:
Received 20 July 2023
Accepted 18 February 2024

Keywords:
Knee osteoarthritis
Axial alignment
Overload
Unloading
Large animal model
Osteochondral unit

SUMMARY

Objective: To investigate whether tibiofemoral alignment influences early knee osteoarthritis (OA). We hypothesized that varus overload exacerbates early degenerative osteochondral changes, and that valgus underload diminishes early OA.

Method: Normal, over- and underload were induced by altering alignment via high tibial osteotomy in adult sheep (n = 8 each). Simultaneously, OA was induced by partial medial anterior meniscectomy. At 6 weeks postoperatively, OA was examined in five individual subregions of the medial tibial plateau using Kellgren-Lawrence grading, quantification of macroscopic OA, semiquantitative histopathological OA and immunohistochemical type-II collagen, ADAMTS-5, and MMP-13 scoring, biochemical determination of DNA and proteoglycan contents, and micro-computed tomographic evaluation of the subchondral bone.

Results: Multivariate analyses revealed that OA cartilaginous changes had a temporal priority over subchondral bone changes. Underload inhibited early cartilage degeneration in a characteristic topographic pattern ($P \geq 0.0983$ vs. normal), in particular below the meniscal damage, avoided alterations of the subarticular spongiosa ($P \geq 0.162$ vs. normal), and prevented the disturbance of otherwise normal osteochondral correlations. Overload induced early alterations of the subchondral bone plate microstructure towards osteopenia, including significantly decreased percent bone volume and increased bone surface–to–volume ratio (all $P \leq 0.0359$ vs. normal).

Conclusion: The data provide high-resolution evidence that tibiofemoral alignment modulates early OA induced by a medial meniscus injury in adult sheep. Since underload inhibits early OA, these data also support the clinical value of strategies to reduce the load in an affected knee compartment to possibly decelerate structural OA progression.

Introduction

Meniscus injury predisposes for early-stage knee osteoarthritis (OA).[1–7] Lower limb alignment in the frontal plane influences the load distribution between the medial and lateral tibiofemoral compartments, modulating OA progression.[8] Varus malalignment with medial overload[9] leads to a higher risk of medial articular cartilage damage and OA.[10] The underloaded compartment displays a reduced risk of incident cartilage damage,[11] loss,[12] and OA.[10,13] Longitudinal clinical studies[10,11,14] or analyses of human late OA[6,13,15,16] confirm the link of malalignment to progressive structural cartilage loss.[17] At mid-term ovine OA, a medial meniscal injury and overload degraded spatial osteochondral trajectories, while underload shifted them

* Correspondence to: Center of Experimental Orthopaedics, Saarland University, Kirrberger Straße 100, Building 37, D-66421 Homburg/Saar, Germany.
E-mail addresses: janreinhard@arcor.de (J. Reinhard), olahtamas@gmail.com (T. Oláh), matthias.laschke@uks.eu (M.W. Laschke), lars.goebel@uks.eu (L.K.H. Goebel), gertrud.schmitt@uniklinikum-saarland.de (G. Schmitt), Susanne-Mentges@arcor.de (S. Speicher-Mentges), michael.menger@uks.eu (M.D. Menger), mmcucchiarini@hotmail.com (M. Cucchiarini), dietrichpape@yahoo.de (D. Pape), henning.madry@uks.eu (H. Madry).
[1] Jan Reinhard and Tamás Oláh contributed equally.

https://doi.org/10.1016/j.joca.2024.02.892

towards normal.[18] For early-stage OA, any potential relationship between over- and underload and its development following a medial meniscal injury remains elusive.

In this study, tibiofemoral alignment was surgically modified to neutral, varus over- and valgus underload in a sheep model of early OA induced by a medial meniscus injury. We hypothesized that overload exacerbates topographic early degenerative osteochondral changes of the medial tibial plateau, and that underload reduces the development of early OA.

Methods

Experimental design

The effects of normal load, varus overload and valgus underload on early OA (Fig. 1A)[18] were investigated at 6 weeks postoperatively. Biplanar osteotomies of the right proximal tibiae (HTO) were performed in adult sheep in a standardized fashion, resulting in neutral alignment, 4.5° tibial varus, and 4.5° tibial valgus, followed by a partial anterior medial meniscectomy (pMMx). The unoperated contralateral left knees served as controls.

At 6 weeks, all animals were euthanized and OA was quantified by radiography, macroscopy, semiquantitative histopathological scoring, immunohistochemistry, biochemistry, and microcomputed-tomography (micro-CT). Reproducibility of micro-CT measurements was confirmed previously.[6] Kellgren-Lawrence (KL) grading of X-ray images was repeated by 2 blinded observers, resulting in similar scores. For histological analysis and semiquantitative scoring, 3 technical repeats (sections) per sample were examined, giving similar results. No outliers or other observations were removed in any of the experimentation shown. Data were always collected blindly and decoded after analysis.

Large animal experiments

Animal experiments were performed according to the German legislation on protection of animals and approved by the Saarland University Animal Committee (43/2015). Sample size (n = 24 sheep) was calculated as described previously.[6,18,19] All left knees served as unoperated controls (n = 24, normal, Supplementary Fig. 1), right knees were randomly assigned into 3 treatment groups: HTO without axial change (n = 8, neutral OA), increased load (n = 8, varus OA) and reduced load (n = 8, valgus OA) (Fig. 1B). Criteria for exclusion were infection or persistent lameness, which no animal met. Following 12 h of fasting, healthy female merino ewes (n = 24, mean age 12–20 months, body weight 70 ± 20 kg, exclusion of radiographic OA) were sedated, received general anesthesia, and underwent surgery.[6,18] Briefly, using an anteromedial approach, a medial biplanar osteotomy of the right proximal tibia was performed and a small stature TomoFix plate fixator (DePuy Synthes, Tuttlingen, Germany) was applied.[18,20–22] Subsequently, the anterior horn of the medial meniscus was resected.[6,18] The joint was rinsed thoroughly, incisions were closed in layers and a spray bandage was applied. Postoperatively, 3 ml of 0.25% fenpipramide/levomethadone (MSD, Unterschleißheim, Germany) and amoxicillin clavulanate (30 mg/kg body weight)(Pfizer, Berlin, Germany) were administered. The following experimental groups with pMMx and HTO were tested: (i) HTO without changing the axial alignment (neutral OA, $n = 8$), (ii) closing wedge HTO inducing 4.5° tibial varus (varus OA, $n = 8$), (iii) opening wedge HTO inducing 4.5° tibial valgus (valgus OA, $n = 8$).[18] The animals were directly allowed full weight bearing. After 6 weeks, ewes were euthanized and the medial tibial plateaus were evaluated.

Radiographic analysis

After resection of the knee joints, anteroposterior radiographs were acquired using an Arcadis Varic image intensifier (Siemens, Erlangen, Germany). Images were evaluated according to the semi-quantitative KL grading system[23] by 2 independent, blinded observers (J.R., L.K.H.G.). Disagreements were resolved by a third observer (H.M.).

Macroscopic grading of OA and definition of topographic subregions

Areas of the medial tibial plateau affected by OA were visualized by India ink staining.[24] The medial tibial plateau was divided into 5 zones to allow for detailed topographic analyses:[6] anterior peripheral and central (each 50% of anterior tibial plateau width), intermediate peripheral and central (40% and 60% of tibial plateau width, respectively), and posterior zone. To acquire standardized pictures a Canon PowerShot A480 camera (Canon, Tokyo, Japan) was used with 50 cm distance to the sample, and standard illumination. CellSens software (Olympus, Hamburg, Germany; version 1.12) was applied for evaluation of the affected area by 2 blinded observers (J.R., T.O.). The severity of OA was graded according to the International Cartilage Regeneration & Joint Preservation Society (ICRS) Cartilage Injury Evaluation Package by a blinded observer (T.O.).[25]

Micro-CT imaging

Ovine tibial plateaus (n = 48 total, including n = 24 controls, n = 8 neutral OA, n = 8 varus OA, n = 8 valgus OA) were scanned in air in a micro-CT scanner (SkyScan 1176, Bruker micro-CT, Kontich, Belgium; 90 kV tube voltage; 278 µA current; 18 µm isotropic resolution; combined 0.5 mm aluminum/copper filter; 0.4° intervals; 270 ms exposure time, 3 averaging frames) and reconstructed with NRecon (v. 1.7.0.4, Bruker micro-CT). After identical rotation of the datasets, coronal images were saved (DataViewer software v. 1.5.2.4, Bruker micro-CT).[6,26]

Volumes of interest (VOIs) of the 5 subregions were marked separately. The following parameters were determined in all VOIs using the software CTAnalyzer (v. 1.16.4.1, Bruker micro-CT): Bone mineral density (BMD), percent bone volume (BV/TV), bone surface–to–volume ratio (BS/BV) and bone surface density (BS/TV). Percentage of closed pores (Po(cl)) were calculated only for the subchondral bone plate. The trabecular thickness (Tb.Th), trabecular separation (Tb.Sp), trabecular number (Tb.N), trabecular pattern factor (Tb.Pf), structure model index (SMI), degree of anisotropy (DA), fractal dimension (FD) and connectivity density (Conn.Dn) were assessed only for the subarticular spongiosa.[6]

Subchondral bone plate and cartilage thickness was measured manually in three-thirds (outer, middle, inner) of each subregion. For 3-dimensional (3D) reconstruction of the micro-CT image sets and modeling of trabecular thickness CTVox v. 3.2.0 (Bruker micro-CT) was used.[26] To generate a 3D model of the porosity of the subchondral bone plate CTVol v. 2.3.2.0 (Bruker micro-CT) was applied.[6] Evaluations were performed by 2 blinded observers (J.R., T.O.).

Semiquantitative histological scoring

Paraffin-embedded samples were sectioned (5 µm) at constant positions corresponding to the previously described regions. A total of 1200 sections (including immunohistochemistry) were analyzed. Safranin O/fast green (n = 720: 3 technical repeats for each of the 5 subregions of n = 24 normal, n = 8 neutral OA, n = 8 varus OA, and n = 8 valgus OA samples) and Masson-Goldner trichrome (n = 240: 1 technical repeat for each of the 5 subregions of n = 24 normal, n = 8 neutral OA, n = 8 varus OA, and n = 8 valgus OA samples) stained

sections[24] were evaluated with the Osteoarthritis Research Society International (OARSI) grades (values increase with OA severity)[27] and stage, modified after Pritzker et al. 2006[27] (based on the extent of macroscopic India ink staining) by 2 blinded observers (J.R., T.O.; mean values were used) selected because of its capability to detect early OA.[28–30] The resulting score equals grade × stage, where stage is the extent of OA: stage 1 < 10%; stage 2 10–25%; stage 3 25–50%; stage 4 > 50% involvement.[27]

Mean values of the analyzed sections were calculated for further analyses. Pictures were obtained with an Olympus BX45 microscope and processed with Photoshop CS5 (Adobe, San Jose, CA, USA).

Immunohistochemistry

Immunohistochemical determination of type-II collagen, ADAMTS-5, and MMP-13 expression was conducted on paraffin-embedded sections (n = 384) using a 1/45 dilution of a monoclonal mouse anti–type-II collagen IgG (AF5710; Acris, Herford, Germany), a 1/50 dilution of a polyclonal rabbit anti–ADAMTS-5 IgG (AB 231595, Abcam, Germany), a 1/100 dilution of a polyclonal rabbit anti–MMP-13 IgG (PA5 - 27242; Invitrogen, Germany), and a biotinylated secondary anti-mouse or anti-rabbit antibody (BA-9200 or BA-1000; Vector Laboratories, Burlingame, CA, USA).[31] A standardized semiquantitative score was used to compare the immunoreactivity to type-II collagen, ADAMTS-5, and MMP-13 in the treated right knees of each animal (score 0 = no immunoreactivity; 1 = weaker; 2 = similar; 3 = stronger immunoreactivity) with that of the corresponding normal left knees serving as an internal control (always score 2), by a blinded observer (J.R. or T.O.).

Biochemical analyses

Cartilage samples were harvested from the anterior part of the intermediate subregions, snap-frozen in liquid nitrogen and stored at −80°C until use. Samples were digested in papain (0.5 mg/ml; overnight at 65°C) to monitor the DNA contents by the Hoechst 33258 fluorometric assay,[32] the proteoglycan contents by binding to dimethyl methylene blue dye (DMMB; Serva, Heidelberg, Germany), and the total cellular protein contents for normalization by using a reliable BCA assay (Pierce BCA Protein Assay Kit, ThermoFisher Scientific, Waltham, MA, USA; #23225).[32] All measurements were performed using a GENios spectrophotometer/fluorometer (Tecan, Männedorf, Switzerland) by a blinded observer (T.O.).

Statistical analysis

To test normal distribution, the Shapiro-Wilk normality test was used. Comparing statistical significance depending on a normal distribution, One Way Analysis of Variance (ANOVA) followed by the Tukey test for all pairwise multiple comparisons or Kruskal-Wallis One Way ANOVA followed by Dunn's test for all pairwise multiple comparisons were used, and multiplicity adjusted *P* values were reported. To test osteochondral correlations, Pearson correlation coefficient (r) was calculated. Heat maps were created with Morpheus (https://software.broadinstitute.org/morpheus). Multivariate analyses were performed for all available bone and cartilage parameters of the relevant individual subregions of the samples as described previously.[6,13] Principal components analysis (PCA) with a variance-covariance matrix routine, hierarchical cluster analysis with Ward's method and Euclidean similarity index, and one-way permutational multivariate analysis of variance (PERMANOVA) with Euclidean similarity index were used, and considering multiplicity issues, the Bonferroni-corrected *P* values were reported.[33] All calculations were performed with Prism v. 8.2.1 (GraphPad Software Inc., San Diego, CA, USA), or Past v. 4.04;[33] $P < 0.05$ was considered statistically significant. Data was expressed as mean ± SD. Box plot diagrams always show the 75th and 25th percentiles (upper and lower borders of the boxes), the minimum and maximum (whiskers), the mean value (+), the median (middle line), and the individual data points (dots).

Results

Early cartilage degeneration is reduced by unloading

After 6 weeks, KL grades ranged from 0 to 2 and were not significantly different between the 4 groups (all $P \geq 0.1315$) (Fig. 1C, D). The anterior subregions displayed the most prominent early OA changes versus normal in all 3 OA groups as determined by macroscopic and microscopic analyses. The anterior central subregion was always predominantly affected (Fig. 1A). When valgus OA was compared with normal, areas affected by macroscopic OA of either the entire medial tibial plateau or the anterior peripheral subregion (Fig. 1A) did not differ significantly ($P \geq 0.0983$) (Fig. 1E). The OA-affected areas within the same subregions of neutral and varus OA knees were always significantly greater than in normal ($P \leq 0.0045$) (Fig. 1E). Significantly less OA was found in the intermediate peripheral region of valgus OA than in that of the normal ($P \leq 0.0383$) and neutral OA groups ($P \leq 0.0447$) (Fig. 1E). Significantly more severe macroscopic cartilage damage in neutral OA developed in the anterior peripheral subregion ($P = 0.0153$), and in all treatment groups in the anterior central subregion ($P \leq 0.0047$) than in normal (Fig. 1F). The histopathological cartilage grades and scores[27] in the anterior peripheral subregions were significantly worse in neutral and varus OA compared to normal ($P \leq 0.0051$) (Fig. 1G-I). The histopathological cartilage structure in valgus OA did not differ significantly from normal ($P = 0.1012$). Mostly unaltered cartilage thickness (Fig. 1J), significantly lower in the peripheral (meniscus-covered) regions compared to the central regions in most groups ($P \leq 0.0288$) (Fig. 1J), and changed biochemical composition, including reduced type-II collagen immunoreactivity in neutral OA compared to all other groups in the anterior central subregion ($P \leq 0.0078$) (Fig. 2A, B) (Supplementary Figs. 2–3) were revealed. Underload resulting from valgus OA caused a lower DNA content in the antero-intermediate central subregion ($P = 0.0036$) (Fig. 2C). Immunoreactivities in the anterior central subregion to ADAMTS-5 were significantly higher in neutral and varus OA versus normal ($P = 0.01$) and significantly lower in valgus versus normal and varus OA ($P = 0.0191$). Immunoreactivities to MMP-13 were significantly higher in neutral and varus OA versus valgus OA ($P \leq 0.0472$) (Fig. 2D-G).

Unloading reverses early OA subchondral bone remodeling

Only varus overload induced a significant early reduction in the percent bone volume (BV/TV) of the subchondral bone plate ($P \leq 0.0218$), together with other microstructural changes, among which bone surface density (BS/TV), bone surface–to–volume ratio (BS/BV), and bone mineral density (BMD) in certain subregions versus normal (all $P \leq 0.0359$) (Fig. 3A-C, Supplementary Fig. 4).

In the subarticular spongiosa, OA both in neutral and varus alignment induced significant ($P \leq 0.0469$) microstructural changes compared to normal (Fig. 3,A, D-G), mostly in the anterior

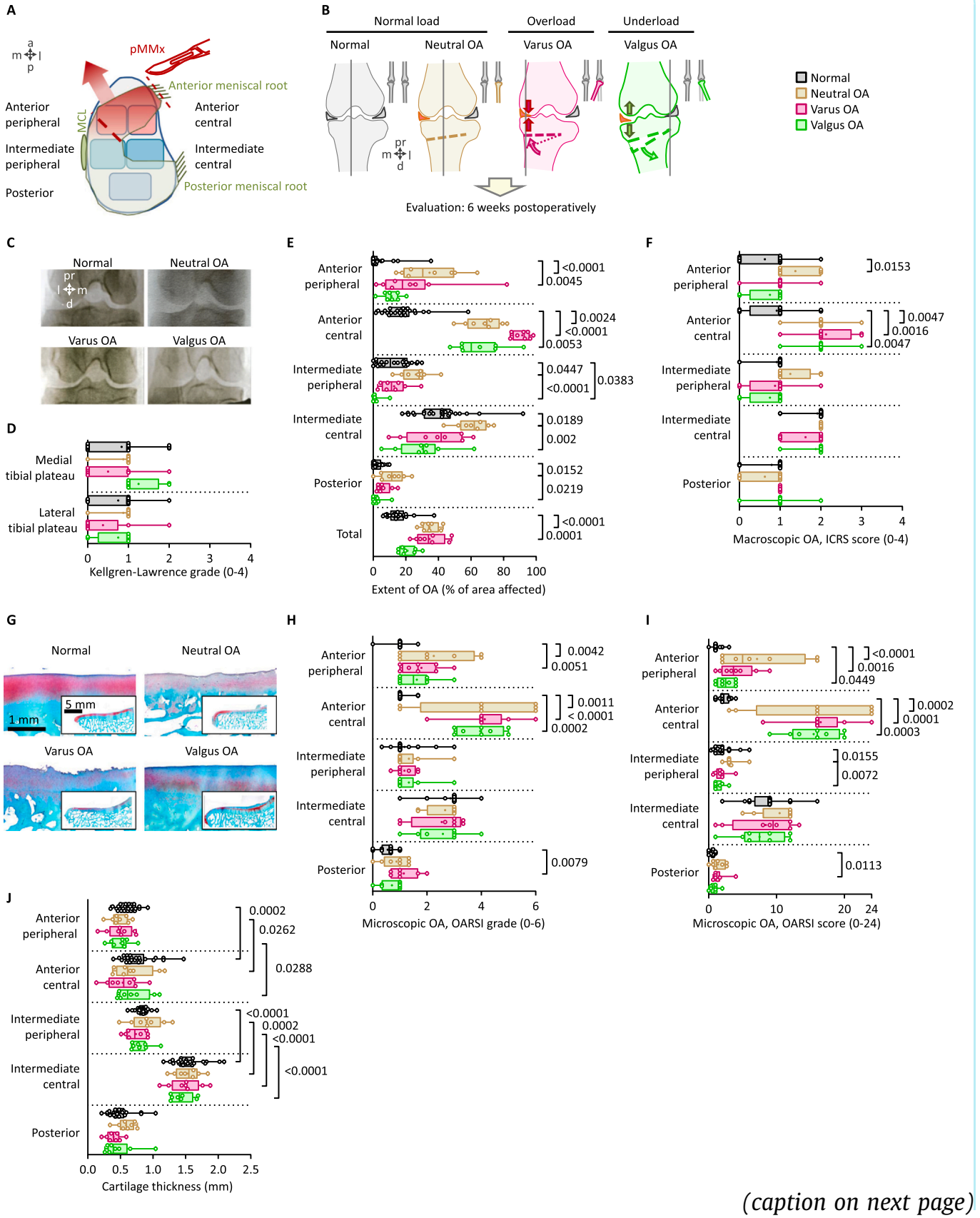

(caption on next page)

Fig. 1 Osteoarthritis and Cartilage

Macroscopic and microscopic osteoarthritic changes of the articular cartilage. **(A)** Effect of partial anterior medial meniscectomy (pMMx; arrow shows the movement of the destabilized meniscus) and subregions in the medial tibial plateau. **(B)** Treatment groups with altered axial alignment. Gray line indicates the weight bearing axis. **(C)** Representative x-ray images (normal is mirrored) and **(D)** Kellgren-Lawrence grades[23] (boxes: 75th-25th percentiles, whiskers: minimum and maximum, middle line: median, +: mean, dots: individual data points). **(E)** Extent of macroscopic OA lesions and **(F)** ICRS grading. **(G)** Representative safranin O stained histological sections from the anterior region, **(H)** OARSI grades[27] and **(I)** OARSI scores.[27] **(J)** Articular cartilage thickness measured with micro-CT. No inter-group differences were detected with ANOVA ($P > 0.05$); peripheral vs. central regional differences were determined with paired T-test or Wilcoxon test. Abbreviations: a, anterior; d, distal; l, lateral; m, medial; MCL, medial collateral ligament; p, posterior; pr, proximal. Normal, n = 24; treatment groups, n = 8 each. *P* values were determined with ANOVA or Kruskal-Wallis ANOVA.

subregions, including significantly lower BV/TV, trabecular thickness (Tb.Th), and fractal dimension (FD) ($P \leq 0.0469$) (Fig. 3B-E), and higher BS/BV ($P \leq 0.0289$) (Fig. 3D-G, Supplementary Fig. 5). As opposed to neutral and varus OA, no significant differences from normal were found in valgus OA in BV/TV, Tb.Th, FD, BS/BV, trabecular pattern factor (Tb.Pf), and structure model index (SMI), (all $P \geq 0.162$) (Fig. 3D-G, Supplementary Fig. 5) in any of the examined subregions.

Multivariate and correlation analyses indicate decelerated early OA following unloading

Principal components analysis (PCA) supported by one-way permutational multivariate analysis of variance (PERMANOVA) of the articular cartilage exposed a clear separation between normal controls and the three treatment groups (all $P = 0.001$) (Fig. 4A, Supplementary Fig. 6). Unloading from valgus OA showed a greater degree of similarity ($F = 13.42$, $P = 0.001$) to normal than neutral and varus OA ($F \geq 18.90$, $P = 0.001$) (Fig. 4A). When subchondral bone parameters were considered, all groups mostly overlapped (Fig. 4B, Supplementary Fig. 6). Although none of the groups differed from each other significantly ($P \geq 0.109$), valgus unloading was also the most similar to normal ($F = 0.84$, $P = 1.000$) (Fig. 4B).

In the combined anterior subregions of normal knees, correlations between the osteochondral parameters were tested without a priori exclusions, and 106 out of the n = 253 comparisons were significant ($P < 0.05$). Seventy of the correlations were significant in neutral OA; 68 in varus OA; and 91 in valgus OA (Fig. 4C). The significant positive correlations between subchondral bone plate and cartilage thickness (Fig. 4D), and subarticular spongiosa BMD and Tb.Th (Fig. 4E), typical features of a normal osteochondral unit ($r = 0.511$ to 0.759, $P \leq 0.0002$), became non-significant in neutral ($r = 0.129$ to 0.388, $P \geq 0.138$) and varus OA ($r = 0.144$ to 0.489, $P \geq 0.055$). In valgus OA such pathological disturbances were prevented ($r = 0.616$ to 0.641, $P \leq 0.011$) (Fig. 4D, E).

Comparison of the early and mid-term patterns of load modulation

Finally, these early effects were compared with the data from a mid-term study (endpoint: 6 months) that was performed previously with an identical study design.[18] In the articular cartilage we observed worse macroscopic ICRS scores and thickening of the articular cartilage at 6 months in the neutral and varus OA groups, while valgus OA prevented such changes (Fig. 5A-C). In the subchondral bone plate, at 6 weeks, reduced thickness and increased bone surface was found mostly in the varus and in some degree at the valgus OA groups, and lower BMD only in the varus OA group. In contrast, at 6 months slightly increased bone mass and reduction of the bone surface and pores was combined with a lower BMD in all groups (Fig. 5A-C).[18] In the subarticular spongiosa, at 6 months, a general loss of trabecular volume and structural complexity was observed in all treatment groups, while at the early, 6 weeks time point these changes only partly developed, and in the valgus unloading group they were mostly completely absent (Fig. 5A-C).

Discussion

This study makes several major contributions to understand how early OA induced by a medial meniscus injury is modulated by tibiofemoral alignment in a clinically relevant ovine model: Early cartilaginous changes have a temporal priority over subchondral bone changes. Overload considerably alters the subchondral bone plate microstructure toward osteopenia (decreased BV/TV, thickness, BMD, and increased BS/BV, BS/TV). Underload inhibits early cartilage degeneration in a characteristic spatial pattern, in particular in the area below the meniscal damage, avoids modifications of the subarticular spongiosa, and prevents the disturbance of otherwise normal osteochondral correlations. When compared with the results at 6 months, unloading prevented the aggravation of the articular cartilage damage, while it was only temporarily capable of altering the pattern of osteoporotic changes in the subarticular spongiosa.

Detailed topographical consequences on both components of the osteochondral unit early after OA induction by a meniscus injury are barely known. In human normal[34] and late OA[35] knees and in normal sheep,[36] a specific topographic pattern of sclerotic subchondral bone and thicker but softer[37] articular cartilage was observed at the meniscus uncovered central areas of the tibial plateau. Moreover, regions of meniscus tissue loss in the tibial plateau of patients with early OA correlated significantly with regions of articular cartilage damage.[6] Here, macroscopic and microscopic OA was more pronounced in the (mostly anterior) central area (Supplementary Fig. 7), suggesting that the remnants of the meniscus retain an ability to protect, as in human OA.[35] Cartilage has been examined after 3 months in sheep after total lateral meniscectomy[38,39] and applying various protocols of medial meniscus injury.[5] The present multivariate analyses indicate that cartilaginous changes have a temporal priority over subchondral bone changes, considering all associated parameters. Many of the physiological correlations between characteristic parameters of the components of the osteochondral unit were already reduced in neutral and varus OA. Interestingly, these changes were undetectable by KL grading, emphasizing the need for precise 3D evaluation methods.[40,41] In (neutral) OA, articular cartilage damage at 6 weeks was characterized by increased expression of the stress-responsive matrix degrading enzymes MMP-13 and ADAMTS-5, loss of matrix staining, surface discontinuity, fissures

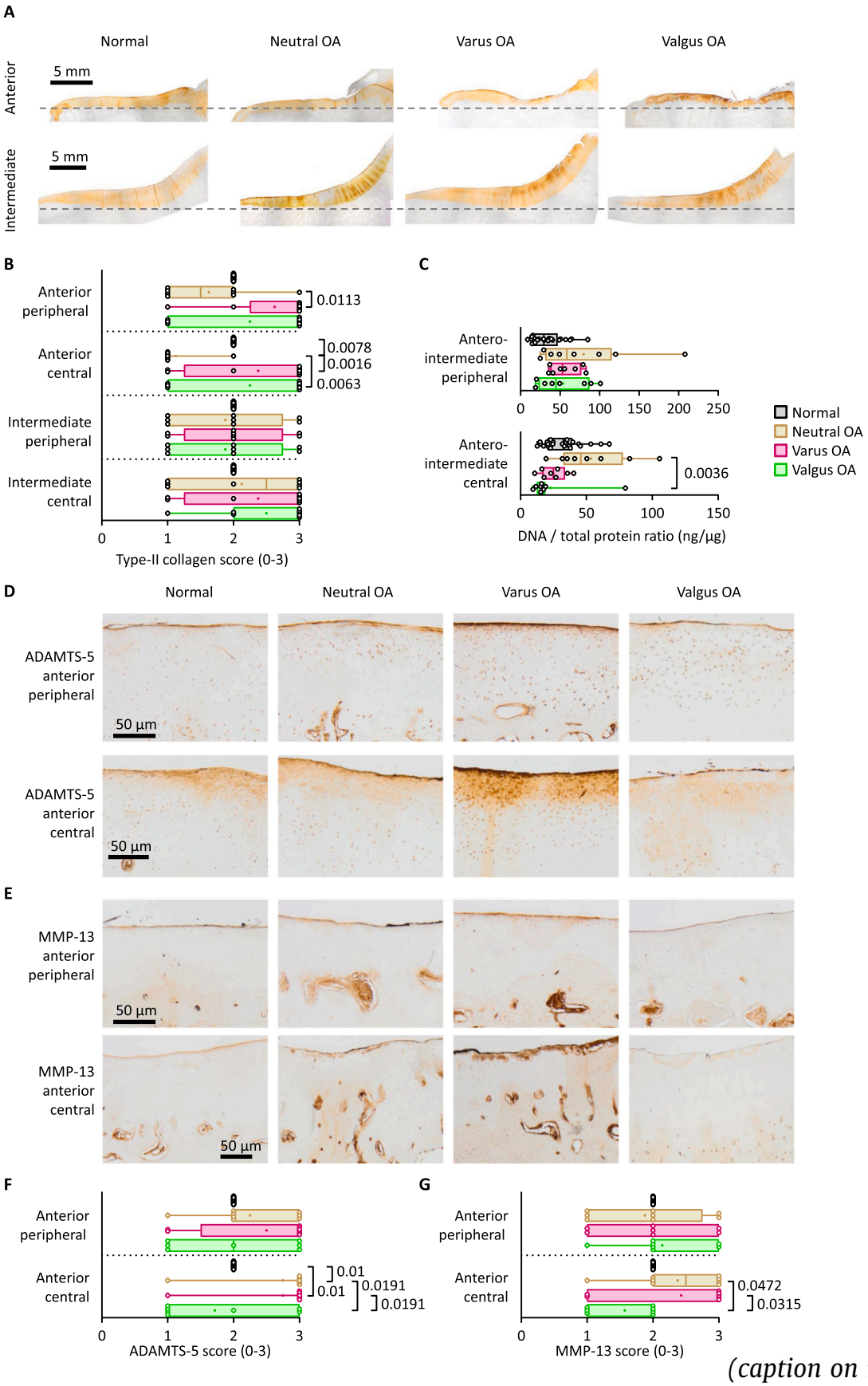

(caption on next page)

Fig. 2

Osteoarthritis and Cartilage

Immunohistochemistry of the articular cartilage. **(A)** Representative immunolabeling of type-II collagen from the anterior and intermediate subregions of normal, neutral OA, varus OA and valgus OA samples. Dashed lines indicate the alignment of the images according to the cement line. **(B)** Type-II collagen scores. **(C)** DNA concentration normalized to the total protein concentration in samples derived from the boundary of the anterior and intermediate subregions. Representative images from the anterior peripheral and central subregions showing immunoreactivity to **(D)** ADAMTS-5 and **(E)** MMP-13. **(F)** ADAMTS-5 and **(G)** MMP-13 scores. Normal, $n = 24$; treatment groups, $n = 8$ each. *P* values were determined with ANOVA or Kruskal-Wallis ANOVA.

(reaching the mid zone) and erosion (in a few samples local denudation; corresponding to OARSI grades ranging between 1–6). Of note, areas with large macroscopic OA (higher OARSI stage) showed an advanced degree of microscopic cartilage degeneration (higher OARSI grade), pronouncing the differences between less and more affected subregions. The subchondral bone microstructure was affected by minor disturbances among which decreased BV/TV, Tb.Th, FD, and increased BS/BV, that developed in the anterior subregion of the subarticular spongiosa, possibly reflecting meniscal instability.

Several clinical studies indicate that malalignment positively correlates with the risk and severity of OA,[10,13] facilitates cartilage thickness loss[17] and accelerates its progression.[11,14,16,42] Importantly, overload alone did not evoke OA without an additional injury of the meniscus in a similar model of modulated alignment.[21,22] Here, overload contributed to a considerably weaker subchondral bone plate microstructure (reflected in decreased BV/TV, thickness, BMD, and increased BS/BV, BS/TV), besides the cartilage changes. Such osteopenic changes may preclude subchondral bone plate sclerosis, an indisputable mark of advanced OA that co-localizes with articular cartilage loss[1,43] and that can be reversed by knee joint distraction (KJD).[44] An osteopenic early OA subchondral bone morphology was reported when examining subregional differences human osteochondral OA specimen without associated bone marrow lesions (OARSI grades ~2–3).[45] It is possible that the increased local contact pressures caused by pMMx lead to the osteopenic subchondral bone plate changes that predispose for subchondral insufficiency fractures, representing an etiological mechanism for osteonecrosis of the knee.[46]

Underload reduced early focal macroscopic and microscopic cartilage damage at 6 weeks, suggesting an immediate beneficial structural effect, similar to findings at 6 months,[18] and normalized expression of MMP-13 and ADAMTS-5. Unloading largely prevented the disturbance of otherwise normal osteochondral correlations. The severe (67% affected area with erosions of OARSI grade 4) development of anterior central OA is likely caused by more meniscal extrusion compared to more posterior subregions which are stabilized by the medial collateral ligament, the posterior root (Fig. 1A) and other structures.[47] Underload did not compensate for these changes, only later at 6 months.[18] Here, in the anterior central subregion, the valgus underload group was significantly worse than normal. It did not differ significantly from neutral OA in macroscopic OA area, ICRS score, microscopic OARSI grade, OARSI score. Underload significantly reduced the pathological cell proliferation occurring in neutral early OA. However, it has to be emphasized that underloading based on reduced physical activity coupled with low body mass index is detrimental for the medial tibiofemoral cartilage.[48] Thus, from a clinical point of view, maintaining physical activity is still necessary to provide for an adequate (dynamic) stimulus to prevent degeneration after reducing the magnitude of load.[49,50] Unloading also prevented degradation of the subarticular spongiosa trabeculae, in contrast to neutral and varus OA. BV/TV, BS/BV, Tb.Pf, SMI, Tb.Th, and FD
of
the subarticular spongiosa were preserved at normal levels in all of the examined subregions upon unloading. These data provide supporting structural evidence for load-altering therapies, among which HTO[51] or KJD.[52]

When early and mid-term[18] results were compared, a worsening articular cartilage degeneration with swelling at mid-term, an increased then decreased bone surface of the subchondral bone plate, related to the changes of its porosity, and a gradually developing general loss of trabecular volume and structural complexity in the subarticular spongiosa were observed in most of the treatment groups, which effects were largely reduced or at least delayed by unloading. Additionally, at 6 weeks, overload evoked similar macroscopic and microscopic OA changes of the articular cartilage, trabecular alterations of the subarticular spongiosa, and anterior loss of osteochondral correlations to neutral OA. This is in contrast to those observed at 6 months, when structural and biochemical changes of the cartilage were more pronounced after overload than in neutral OA.[18] The high similarity of the different alignments at this early phase suggests that the effects of overload develop at a lower velocity.

This study has several limitations. Although the data suggest protective early and mid-term effects of unloading on osteochondral integrity in an early OA-affected compartment,[18] longer-term follow-up is necessary. Considering that sham-operated knees were similar to normal controls,[53] and that sheep undergoing an identical osteotomy without pMMx did not display significant cartilage[21] or subchondral bone changes[22] between operated and non-operated knees, no additional sham-operated controls were included. Based on published evidence[54,55] and the lack of precise tools for measuring loading force in vivo, no data on intraarticular load distribution are provided. Since at the commonly used micro-CT imaging resolutions the calcified cartilage and subchondral cortical bone cannot be separated,[40] a separate histological or high resolution (> 2 μm[56]) micro-CT analysis of these distinct microanatomic structures will be useful in future studies. As the relationship between the amount of antigens and the intensity of immunoreactivity is not stoichiometric,[57] the type-II collagen data should be interpreted with caution. Areas of positive type-II collagen immunoreactivity and safranin O staining were not quantified due to the absence of specific programs allowing to accurately select the articular cartilage. Strengths are the precise inductions of tibiofemoral (mal) alignments in a large animal model highly similar to the clinical situation, 2 control groups including neutral alignment to rule out possible confounding effects of the osteotomy, and the extensive topographical analysis of the entire osteochondral unit at an early time point. Finally, the data support the value of expressing OA both in terms of areal coverage (e.g. OARSI stage) and degree (and depth) of degeneration (e.g. OARSI grade).[27]

In conclusion, we provide high-resolution evidence for the modulation by tibiofemoral alignment of osteochondral changes in early OA induced by a medial meniscus injury in adult sheep, broadening our understanding of this important phase. Since underload inhibits

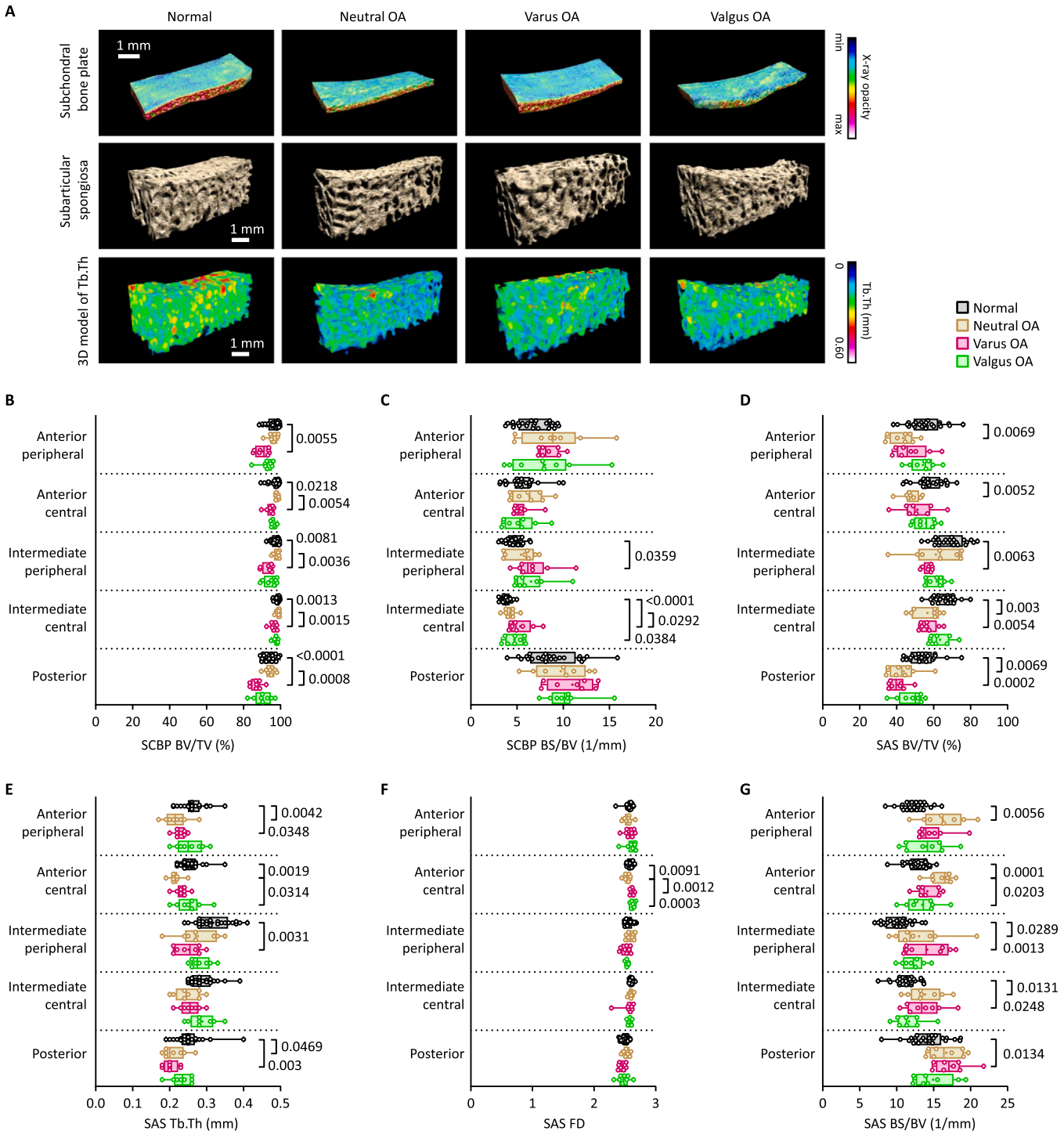

Fig. 3

Osteoarthritis and Cartilage

Structural changes in the subchondral bone. **(A)** Representative 3D reconstructed micro-CT models showing the morphology of the subchondral bone plate, subarticular spongiosa, and color-coding of trabecular thickness of the anterior region. Regional analysis of the **(B)** bone volume fraction (BV/TV), and **(C)** bone surface-to-volume ratio (BS/BV) of the subchondral bone plate (SCBP), and **(D)** BV/TV, **(E)** trabecular thickness (Tb.Th), **(F)** fractal dimension (FD), **(G)** BS/BV of the subarticular spongiosa (SAS). Normal, n = 24; treatment groups, n = 8 each. *P* values above the graphs were determined with ANOVA or Kruskal-Wallis ANOVA.

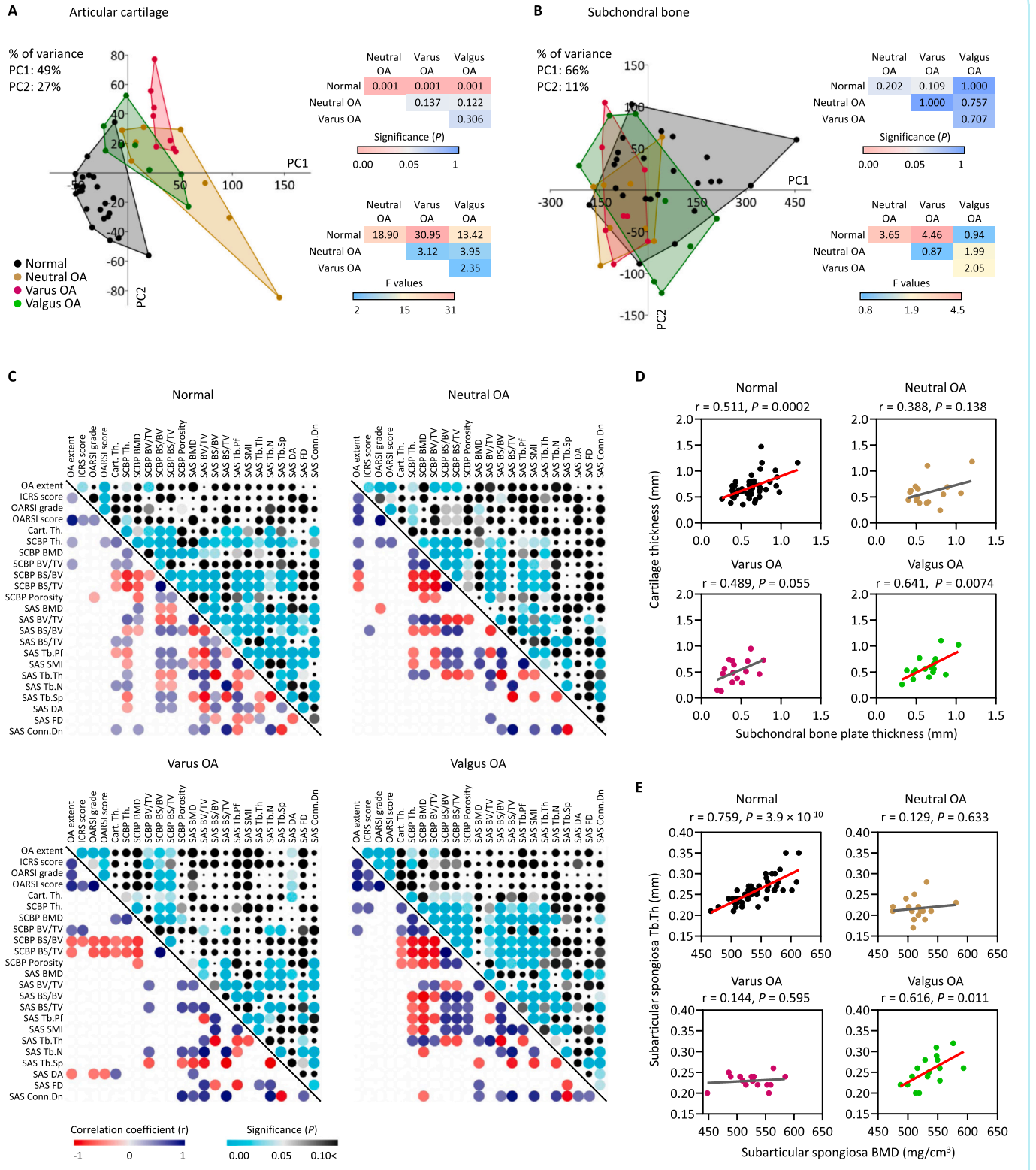

Fig. 4

Osteoarthritis and Cartilage

Multivariate analyses and anterior correlations. Principal components analysis and PERMANOVA of the **(A)** articular cartilage and **(B)** subchondral bone parameters of all subregions. Data points represent individual samples. **(C)** Pearson correlation matrix of the *P* values [decreasing size of dots indicate increasing (less significant) *P* values] and the correlation coefficients (r) of the significant ($P < 0.05$) correlations in the anterior region. Scatter plot and linear regression of the correlation between **(D)** articular cartilage thickness and subchondral bone plate thickness, and **(E)** subarticular spongiosa Tb.Th and BMD in the anterior region. Red regression lines indicate significant ($P < 0.05$) correlations. Normal, n = 24; treatment groups, n = 8.

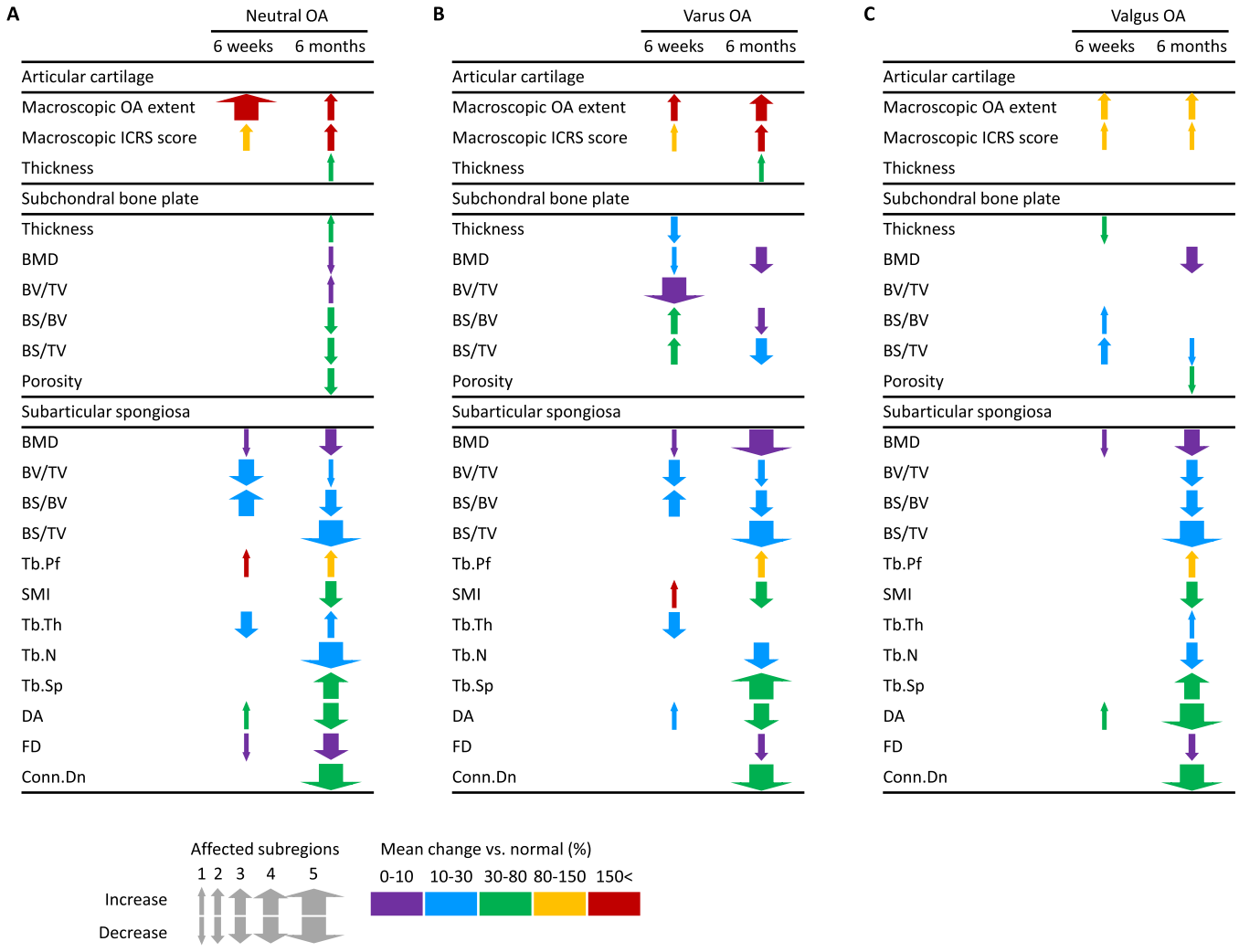

Fig. 5

Osteoarthritis and Cartilage

Comparison of the changes at 6 weeks and 6 months. Data of the present study, showing early OA at 6 weeks, was compared to those of a similar study of mid-term OA at 6 months.[18] Only the significant changes vs. normal are shown in **(A)** neutral OA, **(B)** varus OA, and **(C)** valgus OA. The thickness of the arrows shows the number of affected subregions within the tibial plateau, and the color intensity shows the mean magnitude of the change within the subregions in percentage of the normal (only where $P < 0.05$ vs. normal). Note that the number of affected subregions was always indicated if changes were significant, independently from the degree of change. Normal, n = 24; treatment groups, n = 8 per time point.

early OA, these data also support the clinical value of nonsurgical or surgical strategies to reduce the load in an affected knee compartment to possibly decelerate its structural progression.[58]

Role of the funding source

The funders had no role in the study design, collection, analysis and interpretation of data; in the writing of the manuscript; and in the decision to submit the manuscript for publication.

Author contributions

H.M. conceptualized the study; H.M. and D.P. performed animal surgery; M.W.L. and M.D.M. performed anesthesia; G.S. and S.S.M. performed technical assistance; J.R. and T.O. acquired data; T.O. analyzed data; J.R., T.O., M.C., L.K.H.G. and H.M. interpreted data; T.O., J.R. and H.M. wrote the initial draft. J.R. and T.O. contributed equally to this work. All authors contributed to editing and revising the manuscript, and have approved the submitted version of the manuscript.

Acknowledgements

We thank Liang Gao, Yannik Morscheid, and Ke Tao for their skillful assistance in the animal surgeries. Supported by the German Federal Ministry of Education and Research (BMBF; OVERLOAD-PrevOP: Funding number: 01EC1408C).

Competing interests

H.M. received grants from DFG (German Research Foundation), Deutsche Arthrose-Hilfe, Deutsche Gesellschaft für Orthopädie und Orthopädische Chirurgie, Sorbonne University Paris, and Fidia farmaceutici S.p.A., speaker fees, and travel fees from Novartis and Fidia farmaceutici S.p.A., is a member of the Scientific Advisory Board of Thuasne and Bone therapeutics and received travel fees and was a member of the Scientific Advisory Board of Kolon TissueGene. All other authors declare no competing interests.

Appendix A. Supporting information

Supplementary data associated with this article can be found in the online version at doi:10.1016/j.joca.2024.02.892.

References

1. Goldring SR, Goldring MB. Changes in the osteochondral unit during osteoarthritis: structure, function and cartilage-bone crosstalk. Nat Rev Rheumatol 2016;12:632–44.
2. Hu W, Chen Y, Dou C, Dong S. Microenvironment in subchondral bone: predominant regulator for the treatment of osteoarthritis. Ann Rheum Dis 2021;80:413–22.
3. Englund M, Roemer FW, Hayashi D, *et al.* Meniscus pathology, osteoarthritis and the treatment controversy. Nat Rev Rheumatol 2012;8:412–9.
4. Felson DT. Osteoarthritis as a disease of mechanics. Osteoarthritis Cartilage 2013;21:10–5.
5. Cake MA, Read RA, Corfield G, *et al.* Comparison of gait and pathology outcomes of three meniscal procedures for induction of knee osteoarthritis in sheep. Osteoarthritis Cartilage 2013;21:226–36.
6. Olah T, Reinhard J, Gao L, *et al.* Topographic modeling of early human osteoarthritis in sheep. Sci Transl Med 2019;11, eaax6775.
7. Faucett SC, Geisler BP, Chahla J, *et al.* Meniscus root repair vs meniscectomy or nonoperative management to prevent knee osteoarthritis after medial meniscus root tears: clinical and economic effectiveness. Am J Sports Med 2019;47:762–9.
8. Sharma L, Song J, Felson DT, *et al.* The role of knee alignment in disease progression and functional decline in knee osteoarthritis. JAMA 2001;286:188–95.
9. Moyer RF, Birmingham TB, Chesworth BM, *et al.* Alignment, body mass and their interaction on dynamic knee joint load in patients with knee osteoarthritis. Osteoarthritis Cartilage 2010;18:888–93.
10. Sharma L, Song J, Dunlop D, *et al.* Varus and valgus alignment and incident and progressive knee osteoarthritis. Ann Rheum Dis 2010;69:1940–5.
11. Sharma L, Chmiel JS, Almagor O, *et al.* The role of varus and valgus alignment in the initial development of knee cartilage damage by MRI: the MOST study. Ann Rheum Dis 2013;72:235–40.
12. Moisio K, Chang A, Eckstein F, *et al.* Varus-valgus alignment: reduced risk of subsequent cartilage loss in the less loaded compartment. Arthritis Rheum 2011;63:1002–9.
13. Haberkamp S, Olah T, Orth P, *et al.* Analysis of spatial osteochondral heterogeneity in advanced knee osteoarthritis exposes influence of joint alignment. Sci Transl Med 2020;12, eaba9481.
14. Eckstein F, Wirth W, Hudelmaier M, *et al.* Patterns of femorotibial cartilage loss in knees with neutral, varus, and valgus alignment. Arthritis Rheum 2008;59:1563–70.
15. Chen Y, Hu Y, Yu YE, *et al.* Subchondral trabecular rod loss and plate thickening in the development of osteoarthritis. J Bone Miner Res 2018;33:316–27.
16. Roberts BC, Solomon LB, Mercer G, *et al.* Relationships between in vivo dynamic knee joint loading, static alignment and tibial subchondral bone microarchitecture in end-stage knee osteoarthritis. Osteoarthritis Cartilage 2018;26:547–56.
17. Moyer R, Wirth W, Eckstein F. Longitudinal changes in magnetic resonance imaging-based measures of femorotibial cartilage thickness as a function of alignment and obesity: data from the Osteoarthritis Initiative. Arthritis Care Res (Hoboken) 2017;69:959–65.
18. Olah T, Reinhard J, Laschke MW, *et al.* Axial alignment is a critical regulator of knee osteoarthritis. Sci Transl Med 2022;14, eabn0179.
19. Orth P, Zurakowski D, Alini M, *et al.* Reduction of sample size requirements by bilateral versus unilateral research designs in animal models for cartilage tissue engineering. Tissue Eng Part C Methods 2013;19:885–91.
20. Madry H, Ziegler R, Orth P, *et al.* Effect of open wedge high tibial osteotomy on the lateral compartment in sheep. Part I: analysis of the lateral meniscus. Knee Surg Sports Traumatol Arthrosc 2013;21:39–48.
21. Ziegler R, Goebel L, Cucchiarini M, *et al.* Effect of open wedge high tibial osteotomy on the lateral tibiofemoral compartment in sheep. Part II: standard and overcorrection do not cause articular cartilage degeneration. Knee Surg Sports Traumatol Arthrosc 2014;22:1666–77.
22. Ziegler R, Goebel L, Seidel R, *et al.* Effect of open wedge high tibial osteotomy on the lateral tibiofemoral compartment in sheep. Part III: analysis of the microstructure of the subchondral bone and correlations with the articular cartilage and meniscus. Knee Surg Sports Traumatol Arthrosc 2015;23:2704–14.
23. Kellgren JH, Lawrence JS. Radiological assessment of osteo-arthrosis. Ann Rheum Dis 1957;16:494–502.
24. Orth P, Peifer C, Goebel L, *et al.* Comprehensive analysis of translational osteochondral repair: focus on the histological assessment. Prog Histochem Cytochem 2015;50:19–36.
25. Mainil-Varlet P, Aigner T, Brittberg M, *et al.* Histological assessment of cartilage repair: a report by the Histology Endpoint Committee of the International Cartilage Repair Society (ICRS). J Bone Joint Surg Am 2003;85-A(Suppl 2):45–57.
26. Olah T, Reinhard J, Gao L, *et al.* Reliable landmarks for precise topographical analyses of pathological structural changes of the ovine tibial plateau in 2-D and 3-D subspaces. Sci Rep 2018;8:75.
27. Pritzker KP, Gay S, Jimenez SA, *et al.* Osteoarthritis cartilage histopathology: grading and staging. Osteoarthritis Cartilage 2006;14:13–29.
28. Ylitalo T, Finnila MAJ, Gahunia HK, *et al.* Quantifying complex micro-topography of degenerated articular cartilage surface by contrast-enhanced micro-computed tomography and parametric analyses. J Orthop Res 2019;37:855–66.
29. Kauppinen S, Karhula SS, Thevenot J, *et al.* 3D morphometric analysis of calcified cartilage properties using micro-computed tomography. Osteoarthritis Cartilage 2019;27:172–80.
30. Madry H, Luyten FP, Facchini A. Biological aspects of early osteoarthritis. Knee Surg Sports Traumatol Arthrosc 2012;20:407–22.
31. Orth P, Duffner J, Zurakowski D, *et al.* Small-diameter awls improve articular cartilage repair after microfracture treatment in a translational animal model. Am J Sports Med 2016;44:209–19.
32. Venkatesan JK, Rey-Rico A, Schmitt G, *et al.* rAAV-mediated overexpression of TGF-beta stably restructures human osteoarthritic articular cartilage in situ. J Transl Med 2013;11:211.

33. Hammer Ø, Harper DAT, Ryan PD. PAST: Paleontological statistics software package for education and data analysis. Palaeontologia Electronica 2001;4:1–9.
34. Touraine S, Bouhadoun H, Engelke K, *et al*. Influence of meniscus on cartilage and subchondral bone features of knees from older individuals: a cadaver study. PLoS One 2017;12, e0181956.
35. Mitton G, Engelke K, Uk S, *et al*. A degenerative medial meniscus retains some protective effect against osteoarthritis-induced subchondral bone changes. Bone Reports 2020;12, 100271.
36. Michaelis JC, Olah T, Schrenker S, *et al*. A high-resolution cross-species comparative analysis of the subchondral bone provides insight into critical topographical patterns of the osteochondral unit. Clin Transl Med 2022;12, e745.
37. Appleyard RC, Burkhardt D, Ghosh P, *et al*. Topographical analysis of the structural, biochemical and dynamic biomechanical properties of cartilage in an ovine model of osteoarthritis. Osteoarthritis Cartilage 2003;11:65–77.
38. Cake MA, Read RA, Guillou B, Ghosh P. Modification of articular cartilage and subchondral bone pathology in an ovine meniscectomy model of osteoarthritis by avocado and soya unsaponifiables (ASU). Osteoarthritis Cartilage 2000;8:404–11.
39. Hwa SY, Burkhardt D, Little C, Ghosh P. The effects of orally administered diacerein on cartilage and subchondral bone in an ovine model of osteoarthritis. J Rheumatol 2001;28:825–34.
40. Olah T, Cai X, Gao L, *et al*. Quantifying the human subchondral trabecular bone microstructure in osteoarthritis with clinical CT. Adv Sci (Weinh) 2022;9, e2201692.
41. Eckstein F, Buck R, Wirth W. Location-independent analysis of structural progression of osteoarthritis-taking it all apart, and putting the puzzle back together makes the difference. Semin Arthritis Rheum 2017;46:404–10.
42. Bastick AN, Belo JN, Runhaar J, Bierma-Zeinstra SM. What are the prognostic factors for radiographic progression of knee osteoarthritis? A meta-analysis. Clin Orthop Relat Res 2015;473:2969–89.
43. Jia H, Ma X, Wei Y, *et al*. Loading-induced reduction in sclerostin as a mechanism of subchondral bone plate sclerosis in mouse knee joints during late-stage osteoarthritis. Arthritis Rheumatol 2018;70:230–41.
44. Mastbergen SC, Ooms A, Turmezei TD, *et al*. Subchondral bone changes after joint distraction treatment for end stage knee osteoarthritis. Osteoarthritis Cartilage 2022;30:965–72.
45. Muratovic D, Findlay DM, Cicuttini FM, *et al*. Bone marrow lesions in knee osteoarthritis: regional differences in tibial subchondral bone microstructure and their association with cartilage degeneration. Osteoarthritis Cartilage 2019;27:1653–62.
46. Hussain ZB, Chahla J, Mandelbaum BR, *et al*. The role of meniscal tears in spontaneous osteonecrosis of the knee: a systematic review of suspected etiology and a call to revisit nomenclature. Am J Sports Med 2019;47:501–7.
47. Adili A, Kaneko H, Aoki T, *et al*. Anterior meniscus extrusion is associated with anterior tibial osteophyte width in knee osteoarthritis - The Bunkyo Health Study. Osteoarthr Cartil Open 2023;5, 100364.
48. Voinier D, Neogi T, Stefanik JJ, *et al*. Using cumulative load to explain how body mass index and daily walking relate to worsening knee cartilage damage over two years: the MOST study. Arthritis Rheumatol 2020;72:957–65.
49. Hunter DJ, Eckstein F. Exercise and osteoarthritis. J Anat 2009;214:197–207.
50. Bjerre-Bastos JJ, Nielsen HB, Andersen JR, *et al*. Does moderate intensity impact exercise and non-impact exercise induce acute changes in collagen biochemical markers related to osteoarthritis? - An exploratory randomized cross-over trial. Osteoarthritis Cartilage 2021;29:986–94.
51. Atkinson HF, Birmingham TB, Primeau CA, *et al*. Association between changes in knee load and effusion-synovitis: evidence of mechano-inflammation in knee osteoarthritis using high tibial osteotomy as a model. Osteoarthritis Cartilage 2021;29:222–9.
52. Jansen MP, Mastbergen SC. Joint distraction for osteoarthritis: clinical evidence and molecular mechanisms. Nat Rev Rheumatol 2022;18:35–46.
53. Ghosh P, Sutherland J, Bellenger C, *et al*. The influence of weight-bearing exercise on articular cartilage of meniscectomized joints. An experimental study in sheep. Clin Orthop Relat Res 1990:101–13.
54. Van Thiel GS, Frank RM, Gupta A, *et al*. Biomechanical evaluation of a high tibial osteotomy with a meniscal transplant. J Knee Surg 2011;24:45–53.
55. Willinger L, Lang JJ, Berthold D, *et al*. Varus alignment aggravates tibiofemoral contact pressure rise after sequential medial meniscus resection. Knee Surg Sports Traumatol Arthrosc 2020;28:1055–63.
56. Kerckhofs G, Sainz J, Wevers M, *et al*. Contrast-enhanced nano-focus computed tomography images the cartilage subtissue architecture in three dimensions. Eur Cell Mater 2013;25:179–89.
57. Landini G, Martinelli G, Piccinini F. Colour deconvolution: stain unmixing in histological imaging. Bioinformatics 2021;37:1485–7.
58. Andriacchi TP, Griffin TM, Loeser Jr. RF, *et al*. Bridging Disciplines as a pathway to Finding New Solutions for Osteoarthritis a collaborative program presented at the 2019 Orthopaedic Research Society and the Osteoarthritis Research Society International. Osteoarthr Cartil Open 2020;2, 100026.